IN -34
3814/

NASA Contractor Report 194881

ICASE Report No. 94-10

ICASE

AN ALTERNATIVE ASSESSMENT OF
SECOND-ORDER CLOSURE MODELS IN
TURBULENT SHEAR FLOWS

Charles G. Speziale

Thomas B. Gatsk

USRA   Operated by Universities Space Research Association

ICASE Fluid Mechanics

Due to increasing research being conducted at ICASE in the field of fluid mechanics, future ICASE reports in this area of research will be printed with a green cover. Applied and numerical mathematics reports will have the familiar blue cover, while computer science reports will have yellow covers. In all other aspects the reports will remain the same; in particular, they will continue to be submitted to the appropriate journals or conferences for formal publication.
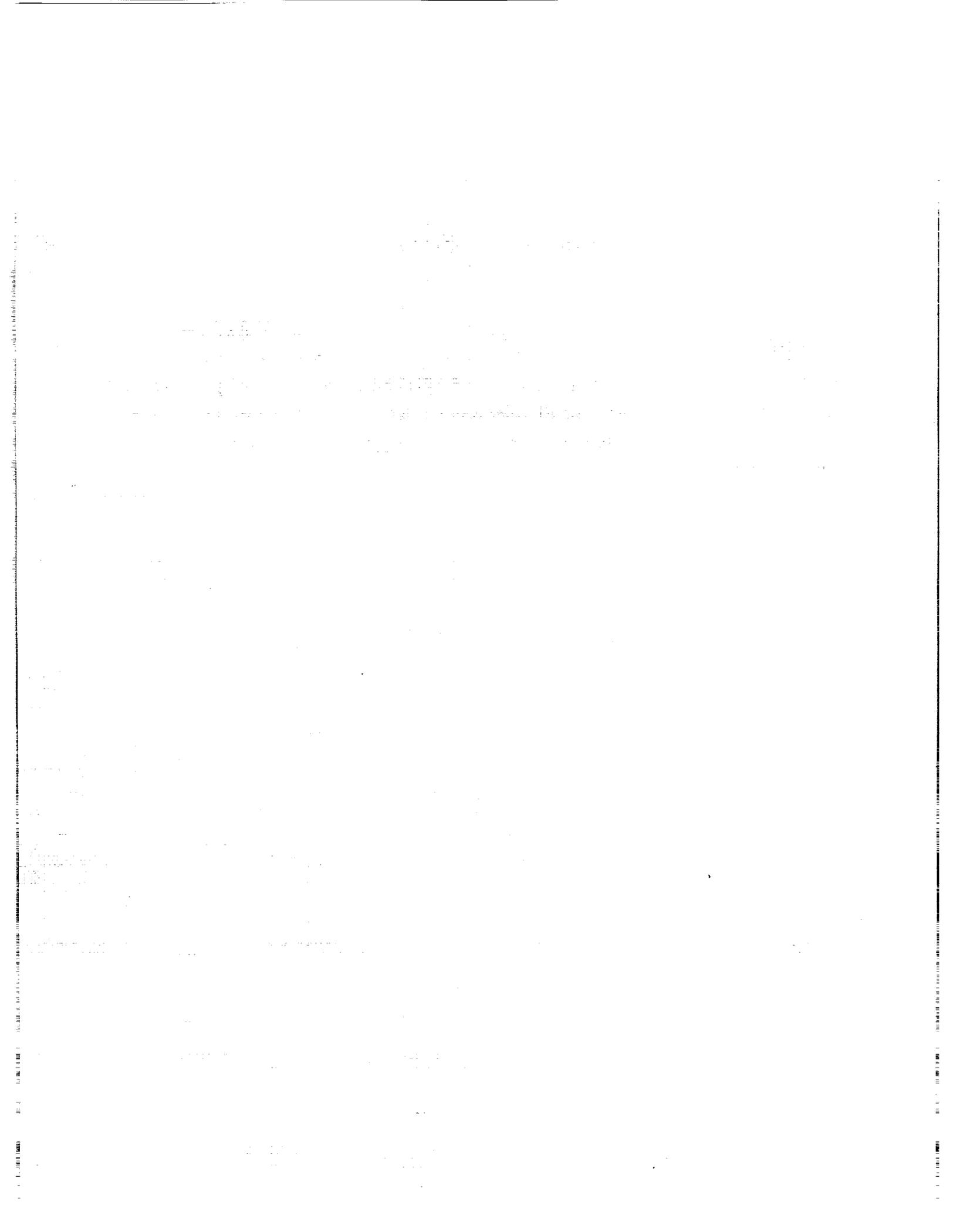
AN ALTERNATIVE ASSESSMENT OF
SECOND-ORDER CLOSURE MODELS IN
TURBULENT SHEAR FLOWS

Charles G. Speziale*

Aerospace & Mechanical Engineering Department

Boston University

Boston, Massachusetts 02215

Thomas B. Gatski

NASA Langley Research Center

Hampton, Virginia 23681

ABSTRACT

The performance of three recently proposed second-order closure models is tested in benchmark turbulent shear flows. Both homogeneous shear flow and the log-layer of an equilibrium turbulent boundary layer are considered for this purpose. An objective analysis of the results leads to an assessment of these models that stands in contrast to that recently published by other authors. A variety of pitfalls in the formulation and testing of second-order closure models are uncovered by this analysis.

INTRODUCTION

The need for advanced turbulence models to reliably compute the complex aerodynamic flows of technological interest has led to a resurgence of interest in second-order closure models. Consequently, the recent papers by Shih, Chen and Lumley[1] and Shih and Lumley[2], which reported tests of second-order closure models in turbulent shear flows, attracted our attention. In these papers, results were presented which appear to indicate that the Shih-Lumley model[3] performs better than other recently proposed second-order closures in homogeneous shear flow as well as in other boundary-free turbulent shear flows. However, our own comparative studies of second-order closure models in benchmark turbulent shear flows have yielded a different picture. The purpose of the current paper is to present these alternative results for comparison.

The predictions of three second-order closure models recently proposed by Shih and Lumley[2,3], Fu, Launder and Tselepidakis[4] and Speziale, Sarkar and Gatski[5] will be compared in two benchmark turbulent flows: homogeneous shear flow and the log-layer of an equilibrium turbulent boundary layer. These flows are selected since the former constitutes a basic building-block free turbulent shear flow whereas the latter serves as a cornerstone for the calculation of practical wall-bounded turbulent flows of engineering interest. Particular attention will be paid to evaluating the ability of each model to accurately predict the equilibrium values for the Reynolds stress anisotropies. However, for the case of homogeneous shear flow, model predictions for time evolving fields will also be compared. Objective means for evaluating the performance of the models will be provided and pitfalls in the formulation and evaluation of models are uncovered that have led to previously published assessments that are misleading.

THE TURBULENT SHEAR FLOWS TO BE CONSIDERED

We will consider incompressible turbulent shear flows with the mean velocity gradient tensor

$$\frac{\partial \overline{v}_i}{\partial x_j} = S \delta_{i1} \delta_{j2} \tag{1}$$

where δ_{ij} is the Kronecker delta and S is shear rate. In homogeneous shear flow, the shear rate S is constant and is applied in an unbounded flow domain yielding spatially homogeneous turbulence statistics. For this, as well as any homogeneous turbulence, the Reynolds stress tensor τ_{ij} is a solution of the transport equation[6]

$$\dot{\tau}_{ij} = -\tau_{ik} \frac{\partial \overline{v}_j}{\partial x_k} - \tau_{jk} \frac{\partial \overline{v}_i}{\partial x_k} + \Phi_{ij} - \varepsilon_{ij} \tag{2}$$

1

where $\tau_{ij} \equiv \overline{u_i u_j}$ and

$$\Phi_{ij} = \overline{p\left(\frac{\partial u_i}{\partial x_j} + \frac{\partial u_j}{\partial x_i}\right)}, \quad \varepsilon_{ij} = 2\nu\overline{\frac{\partial u_i}{\partial x_k}\frac{\partial u_j}{\partial x_k}} \tag{3}$$

are, respectively, the pressure-strain correlation and dissipation rate tensor (here, p is the fluctuating pressure, u_i is the fluctuating velocity, ν is the kinematic viscosity, and an overbar represents an ensemble mean). Since

$$\Phi_{ij} - \varepsilon_{ij} = \Pi_{ij} - \frac{2}{3}\varepsilon\delta_{ij} \tag{4}$$

where $\Pi_{ij} \equiv \Phi_{ij} - {}_D\varepsilon_{ij}$ given that ${}_D\varepsilon_{ij}$ is the deviatoric part of the dissipation rate tensor ($\varepsilon \equiv \frac{1}{2}\varepsilon_{ii}$), closure is achieved once models for Π_{ij} and ε are provided. In most existing second-order closure models, ${}_D\varepsilon_{ij}$ is neglected while Π_{ij} and ε are modeled in the general form:

$$\Pi_{ij} = \varepsilon\mathcal{A}_{ij}(\boldsymbol{b}) + K\mathcal{M}_{ijkl}(\boldsymbol{b})\frac{\partial\overline{v}_k}{\partial x_l} \tag{5}$$

$$\dot{\varepsilon} = -C_{\varepsilon 1}\frac{\varepsilon}{K}\tau_{ij}\frac{\partial\overline{v}_i}{\partial x_j} - C_{\varepsilon 2}\frac{\varepsilon^2}{K} \tag{6}$$

where

$$K = \frac{1}{2}\tau_{ii}, \quad b_{ij} = \frac{\tau_{ij} - \frac{2}{3}K\delta_{ij}}{2K} \tag{7}$$

are the turbulent kinetic energy and Reynolds stress anisotropy tensor, respectively. Here, $\mathcal{A}_{ij}$ and $\mathcal{M}_{ijkl}$ are dimensionless tensor functions of b_{ij} and possibly the turbulence Reynolds number $R_t \equiv K^2/\nu\varepsilon$; $C_{\varepsilon 1}$ and $C_{\varepsilon 2}$ are either constants or functions of the second and third invariants (II, III) of b_{ij} as well as R_t. The full form of the three models to be considered – the Shih-Lumley (SL) model, the Fu, Launder and Tselepidakis (FLT) model and the Speziale, Sarkar and Gatski (SSG) model – are provided in the Appendix.

For homogeneous shear flow, each of the models – consistent with physical and numerical experiments – predict that the anisotropy tensor b_{ij} and shear parameter SK/ε achieve equilibrium values that are independent of the initial conditions (see Tavoularis and Corrsin[7], Rogers, Moin and Reynolds[8] and Tavoularis and Karnik[9]). This equilibrium state is associated with solutions where $\dot{b}_{ij} = 0$ or equivalently,

$$\dot{\tau}_{ij} = (\mathcal{P} - \varepsilon)\frac{\tau_{ij}}{K} \tag{8}$$

where $\mathcal{P} = -\tau_{ij}\partial\overline{v}_i/\partial x_j$ is the turbulence production. The substitution of (1) and (8) into (2) yields the system of algebraic equations (see Abid and Speziale[10])

$$-\frac{\tau_{ij}}{K}\frac{\tau_{12}}{K}\left(\frac{\mathcal{P}/\varepsilon - 1}{\mathcal{P}/\varepsilon}\right) = -\frac{\tau_{i2}}{K}\delta_{j1} - \frac{\tau_{j2}}{K}\delta_{i1} + \Pi_{ij}^* + \frac{2}{3}\frac{\tau_{12}}{K}\left(\frac{\mathcal{P}}{\varepsilon}\right)^{-1}\delta_{ij} \tag{9}$$

2

where $\Pi_{ij}^* \equiv \Pi_{ij}/SK$ is, for the turbulent shear flows to be considered, a function of τ_{ij}/K and $\mathcal{P}/\varepsilon$ whose specific form depends on the pressure-strain model chosen. In deriving (9), the identity

$$\frac{\mathcal{P}}{\varepsilon} = -\frac{\tau_{12}}{K}\left(\frac{SK}{\varepsilon}\right) \tag{10}$$

has been used. Once the equilibrium value of $\mathcal{P}/\varepsilon$ is specified (and Eq. (7) is utilized), it is straightforward to obtain the equilibrium values of b_{ij} from a numerical solution of (9). These equilibrium values are *determined exclusively by the pressure-strain model.*

In the logarithmic region of an equilibrium turbulent boundary layer, the mean velocity gradient tensor is of the general form (1) and there is a production-equals-dissipation equilibrium where the turbulent diffusion terms vanish in the Reynolds stress transport equation. Consequently, (9) yields the equilibrium Reynolds stress anisotropies for the log-layer when $\mathcal{P}/\varepsilon = 1$ (see Abid and Speziale[10]). In contrast to this, homogeneous shear flow achieves an equilibrium state where $\mathcal{P}/\varepsilon > 1$ (physical and numerical experiments[7-9] have indicated that $1.4 \leq \mathcal{P}/\varepsilon \leq 1.8$).

DISCUSSION OF RESULTS

A comparison of the results predicted by the pressure-strain models of Shih and Lumley[2,3], Fu, Launder and Tselepidakis[4] and Speziale, Sarkar and Gatski[5] will now be made. In Figures 1(a) and 1(b), the model predictions for the norm of the slow and rapid parts of the pressure-strain correlation are compared with the DNS results of Rogers, Moin and Reynolds[8] for homogeneous shear flow ($\Pi_{ij} \equiv \Pi_{ij}^{(S)} + \Pi_{ij}^{(R)}$ where the superscripts (S) and (R) denote, respectively, the slow and rapid parts; $(\Pi_{ij}\Pi_{ij})^{1/2}$ denotes the L_2 norm of Π_{ij})). These results are similar to those used by Shih and Lumley[2] to conclude that the Shih-Lumley model performs the best of these three models and that the SSG model performs poorly. Such a conclusion is highly misleading. The SSG model is a model for the *total* pressure-strain correlation and not for its separate slow and rapid parts. The standard hierarchy of pressure-strain models (5) are only theoretically justified for homogeneous turbulent flows that are near equilibrium (as shown by Speziale, Gatski and Sarkar[11], both the slow and rapid parts of the pressure-strain correlation depend nonlinearly on the mean velocity gradients at retarded times in non-equilibrium turbulent flows). When (5) is thought of as the simplified equilibrium form of a more general pressure-strain model it becomes ambiguous as to which part of (5) represents the slow pressure-strain and which part of (5) represents the rapid pressure-strain. It can only be said definitively that $\varepsilon \mathcal{A}_{ij}$ is the slow pressure-strain in the limit of relaxational turbulent flows and that $K\mathcal{M}_{ijkl}\partial \overline{v}_k/\partial x_l$ is the rapid pressure-strain in the rapid distortion limit.[11] This ambiguity causes no problem since only the *total* pressure-

3

strain correlation is needed in (2) for the calculation of the Reynolds stresses. When the model predictions for the norm of the total pressure-strain correlation are compared with the DNS of Rogers *et al.*[8] for homogeneous shear flow a rather different picture emerges as can be seen in Figure 1(c). The SSG model performs as well, if not better, than the SL and FLT pressure-strain models. Furthermore, it was shown by Speziale, Sarkar and Gatski[11] that none of the other models are capable of predicting the individual slow or rapid parts of the pressure-strain correlation for a wide range of homogeneous turbulent flows. The results presented in Shih and Lumley[2] are misleading in this regard.

Comparisons such as those shown in Figure 1 are not very helpful for determining the predictive capabilities of a pressure-strain model in turbulent shear flows. A better test for gauging the performance of a model is to determine its ability to predict accurate equilibrium values for the Reynolds stress anisotropies. These are the crucial physical quantities in homogeneous shear flow that are independent of the initial conditions and, therefore, *repeatable*. Over thirty independent test runs of homogeneous shear flow in reported physical and numerical experiments[7-9] have yielded equilibrium values for the Reynolds stress anisotropies that lie within 10% of one another. On the other hand, the time evolutions of the individual Reynolds stresses vary by factors of 3 or 4 depending on the initial conditions of the test case.

In Table 1, the equilibrium Reynolds stress anisotropies predicted by the SL, FLT and SSG models are compared with the experimental results for homogeneous shear flow for $\mathcal{P}/\varepsilon = 1.5$. This value of $\mathcal{P}/\varepsilon$ is chosen since it is the average value obtained from the most recent experiments. The SSG model is in closest agreement with the experimental data whereas the SL model exhibits the largest discrepancies. The same trend is exhibited for other equilibrium values of $\mathcal{P}/\varepsilon$ in the experimental range of 1.4 - 1.8 (see Abid and Speziale[10] for more details).

As discussed earlier, the equilibrium Reynolds stress anisotropies for the log-layer of a two-dimensional turbulent boundary layer can be obtained from (9), after setting $\mathcal{P}/\varepsilon = 1$. The results obtained from the SL, FLT and SSG models are compared with experimental data[12,13] in Table 2. The results obtained are similar to those obtained for homogeneous shear flow: the SSG model is in the closest agreement with the experimental data while the SL model exhibits the largest deviations. In regard to the latter point, it is surprising how poorly the SL model performs in its prediction of the normal Reynolds stress anisotropies.

In Figure 2, the model predictions for the time evolution of the turbulent kinetic energy in homogeneous shear flow are shown for two test cases: the large-eddy simulation (LES) of Bardina et al.[14] and the DNS of Rogers et al.[8] (run C128X). Here, the dimensionless turbulent kinetic energy and dimensionless time are given by $K^* \equiv K/K_0$ and $t^* = St$,

4

respectively. These results exhibit the same trend as before: the SSG model performs the best and the SL model has the largest deviations. The low growth rate predicted by the SL model arises from its underprediction of the equilibrium value of b_{12} (see Table 1).

This brings us to the basic question as to why the SL model performs poorly in these simple shear flows. As discussed in Shih et al.[1], the SL model was, to a large extent, calibrated based on realizability constraints. It was recently shown by Speziale, Abid and Durbin[15] that the SL model yields *unrealizable* results in homogeneous shear flow due to an error in their analysis. In Figure 3, the time evolution of the invariant function $F \equiv 1 + 9II + 27III$ predicted by each model in homogeneous shear flow is shown for the anisotropic initial conditions: $b_{11} = -0.32$, $b_{22} = b_{33} = 0.16$, $b_{12} = b_{23} = b_{13} = 0$, and $SK/\varepsilon = 15$. For realizable turbulence, we must have $F \geq 0$. It is clear that for these initial conditions, the FLT and SSG models yield realizable solutions whereas the SL model yields unrealizable results! Hence the primary theoretical constraint by which the SL model was formulated is in error.

In conclusion, it must be said that the good performance of a model in these basic turbulent shear flows is no guarantee that it will perform well in more complex turbulent flows. However, these simple test flows do bear directly on how well a model will perform in equilibrium turbulent boundary layers which form a cornerstone for many engineering applications. A model that cannot predict these simple test cases accurately should be abandoned for use in more complex engineering flows.

APPENDIX

The detailed form of the turbulence models considered in the paper are as follows:

Shih & Lumley Model

$$
\begin{aligned}
\Pi_{ij} = & -C_1\varepsilon b_{ij} + \frac{4}{5}K\overline{S}_{ij} + 12\alpha_5 K\left(b_{ik}\overline{S}_{jk} + b_{jk}\overline{S}_{ik}\right. \\
& \left. -\frac{2}{3}b_{kl}\overline{S}_{kl}\delta_{ij}\right) + \frac{4}{3}(2 - 7\alpha_5)K(b_{ik}\overline{\omega}_{jk} + b_{jk}\overline{\omega}_{ik}) \\
& +\frac{4}{5}K(b_{il}b_{lm}\overline{S}_{jm} + b_{jl}b_{lm}\overline{S}_{im} - 2b_{ik}\overline{S}_{kl}b_{lj} \\
& -3b_{kl}\overline{S}_{kl}b_{ij}) + \frac{4}{5}K(b_{il}b_{lm}\overline{\omega}_{jm} + b_{jl}b_{lm}\overline{\omega}_{im})
\end{aligned}
\tag{A1}
$$

$$
C_1 = 2 + \frac{F}{9}\exp(-7.77/\sqrt{Re_t})\{72/\sqrt{Re_t} + 80.1\, ln[1 + 62.4(-II + 2.3III)]\}
\tag{A2}
$$

$$
F = 1 + 9II + 27III
\tag{A3}
$$

$$
II = -\frac{1}{2}b_{ij}b_{ij}, \quad III = \frac{1}{3}b_{ij}b_{jk}b_{ki}
\tag{A4}
$$

$$
Re_t = \frac{4}{9}\frac{K^2}{\nu\varepsilon}
\tag{A5}
$$

$$
\alpha_5 = \frac{1}{10}\left(1 + \frac{4}{5}F^{\frac{1}{2}}\right)
\tag{A6}
$$

$$
C_{\varepsilon 1} = 1.20, \quad C_{\varepsilon 2} = \frac{7}{5} + 0.49\exp(-2.83/\sqrt{Re_t})[1 - 0.33ln(1 - 55II)]
\tag{A7}
$$

Fu, Launder & Tselepidakis Model

$$
\begin{aligned}
\Pi_{ij} = & -C_1\varepsilon b_{ij} + C_2\varepsilon\left(b_{ik}b_{kj} - \frac{1}{3}b_{kl}b_{kl}\delta_{ij}\right) \\
& +\frac{4}{5}K\overline{S}_{ij} + 1.2K\left(b_{ik}\overline{S}_{jk} + b_{jk}\overline{S}_{ik} - \frac{2}{3}b_{kl}\overline{S}_{kl}\delta_{ij}\right) \\
& +\frac{26}{15}K(b_{ik}\overline{\omega}_{jk} + b_{jk}\overline{\omega}_{ik}) + \frac{4}{5}K(b_{ik}b_{kl}\overline{S}_{jl} \\
& +b_{jk}b_{kl}\overline{S}_{il} - 2b_{ik}\overline{S}_{kl}b_{lj} - 3b_{kl}\overline{S}_{kl}b_{ij}) \\
& +\frac{4}{5}K\left(b_{ik}b_{kl}\overline{\omega}_{jl} + b_{jk}b_{kl}\overline{\omega}_{il}\right) - \frac{14}{5}K\left[8II(b_{ik}\overline{\omega}_{jk}\right. \\
& \left. +b_{jk}\overline{\omega}_{ik}) + 12\left(b_{ik}b_{kl}\overline{\omega}_{lm}b_{mj} + b_{jk}b_{kl}\overline{\omega}_{lm}b_{mi}\right)\right]
\end{aligned}
\tag{A8}
$$

6

$$C_1 = -120 II\sqrt{F} - 2\sqrt{F} + 2, \quad C_2 = 144 II\sqrt{F} \tag{A9}$$

$$C_{\epsilon 1} = 1.44, \ C_{\epsilon 2} = 1.90 \tag{A10}$$

Speziale, Sarkar & Gatski Model

$$\Pi_{ij} = -(C_1\epsilon + C_1^*\mathcal{P})b_{ij} + C_2\epsilon\left(b_{ik}b_{kj} - \frac{1}{3}b_{kl}b_{kl}\delta_{ij}\right) + (C_3 - C_3^*II_b^{\frac{1}{2}})K\overline{S}_{ij}$$

$$+ C_4K\left(b_{ik}\overline{S}_{jk} + b_{jk}\overline{S}_{ik} - \frac{2}{3}b_{kl}\overline{S}_{kl}\delta_{ij}\right) + C_5K(b_{ik}\overline{\omega}_{jk} + b_{jk}\overline{\omega}_{ik}) \tag{A11}$$

$$C_1 = 3.4, \ C_1^* = 1.80, \ C_2 = 4.2, \ C_3 = \frac{4}{5}, \ C_3^* = 1.30, \ C_4 = 1.25, \ C_5 = 0.40 \tag{A12}$$

$$II_b = b_{ij}b_{ij} \tag{A13}$$

$$C_{\epsilon 1} = 1.44, \ C_{\epsilon 2} = 1.83. \tag{A14}$$

In these models, $\overline{S}_{ij}$ and $\overline{\omega}_{ij}$ are, respectively, the symmetric and antisymmetric parts of the mean velocity gradient tensor $\partial\overline{v}_i/\partial x_j$ which are given by

$$\overline{S}_{ij} = \frac{1}{2}\left(\frac{\partial\overline{v}_i}{\partial x_j} + \frac{\partial\overline{v}_j}{\partial x_i}\right), \tag{A15}$$

$$\overline{\omega}_{ij} = \frac{1}{2}\left(\frac{\partial\overline{v}_i}{\partial x_j} - \frac{\partial\overline{v}_j}{\partial x_i}\right). \tag{A16}$$

REFERENCES

1. Shih, T. H., Chen, J. Y. and Lumley, J. L., "Second-Order Modeling of Boundary-Free Turbulent Shear Flows," *AIAA J.* Vol. 30, 1992, pp. 1553-1560.

2. Shih, T. H. and Lumley, J. L., "Critical Comparison of Second-Order Closures with Direct Numerical Simulations of Homogeneous Turbulence," *AIAA J.* Vol. 31, 1993, pp. 663-670.

3. Shih, T. H. and Lumley, J. L., "Modeling of Pressure Correlation Terms in Reynolds Stress and Scalar Flux Equations," *Cornell University Technical Report FDA-85-3*, 1985.

4. Fu, S., Launder, B. E. and Tselepidakis, D. P., "Accommodating the Effects of High Strain Rates in Modeling the Pressure-Strain Correlation," *UMIST Technical Report TFD/87/5*, 1987.

5. Speziale, C. G., Sarkar, S. and Gatski, T. B., "Modeling the Pressure-Strain Correlation of Turbulence: An Invariant Dynamical Systems Approach," *J. Fluid Mech.* Vol. 227, 1991, pp. 245-272.

6. Hinze, J. O., *Turbulence*, McGraw-Hill, New York, 1975.

7. Tavoularis, S. and Corrsin, S., "Experiments in Nearly Homogeneous Turbulent Shear Flow with a Uniform Mean Temperature Gradient. Part I," *J. Fluid Mech.* Vol. 104, 1981, pp. 311-347.

8. Rogers, M. M., Moin, P. and Reynolds, W. C., "The Structure and Modeling of the Hydrodynamic and Passive Scalar Fields in Homogeneous Turbulent Shear Flow," *Stanford University Technical Report TF-25*, 1986.

9. Tavoularis, S. and Karnik, U., "Further Experiments on the Evolution of Turbulent Stresses and Scales in Uniformly Sheared Turbulence," *J. Fluid Mech.* Vol. 204, 1989, pp. 457-478.

10. Abid, R. and Speziale, C. G., "Predicting Equilibrium States with Reynolds Stress Closures in Channel Flow and Homogeneous Shear Flow," *Phys. Fluids A* Vol. 5, 1993, pp. 1776-1782.

11. Speziale, C. G., Gatski, T. B. and Sarkar, S., "On Testing Models for the Pressure-Strain Correlation of Turbulence using Direct Simulations," *Phys. Fluids A* Vol. 4, 1992, pp. 2887-2899.

12. Klebanoff, P. S., "Characteristics of Turbulence in a Boundary Layer with Zero Pressure Gradient," *NACA TN 3178*, 1956.

13. Laufer, J., "Investigation of Turbulent Flow in a Two-Dimensional Channel," *NACA Technical Report 1053*, 1951.

14. Bardina, J., Ferziger, J. H. and Reynolds, W. C., "Improved Turbulence Models Based on Large-Eddy Simulation of Homogeneous Incompressible Turbulent Flows," *Stanford University Technical Report TF-19*, 1983.

15. Speziale, C. G., Abid, R. and Durbin, P. A., "New Results on the Realizability of Reynolds Stress Turbulence Closures," *ICASE Report 93-76*, NASA Langley Research Center, 1993.

Equilibrium Values	SL Model	FLT Model	SSG Model	Experimental Data
b_{11}	0.105	0.177	0.214	0.20 to 0.21
b_{12}	−0.121	−0.157	−0.163	−0.14 to −0.16
b_{22}	−0.107	−0.122	−0.140	−0.14 to −0.15
b_{33}	0.002	−0.055	−0.074	−0.05 to −0.07

Table 1. Equilibrium Reynolds stress anisotropies in homogeneous shear flow: Comparison of the model predictions with physical and numerical experiments.[7-9]

Equilibrium Values	SL Model	FLT Model	SSG Model	Experimental Data
b_{11}	0.079	0.141	0.201	0.20 to 0.23
b_{12}	−0.116	−0.162	−0.160	−0.14 to −0.16
b_{22}	−0.082	−0.099	−0.126	−0.13 to −0.15
b_{33}	0.003	−0.042	−0.075	−0.05 to −0.10

Table 2. Reynolds stress anisotropies in the log-layer of an equilibrium turbulent boundary layer: Comparison of the model predictions with experiments.[12-13]
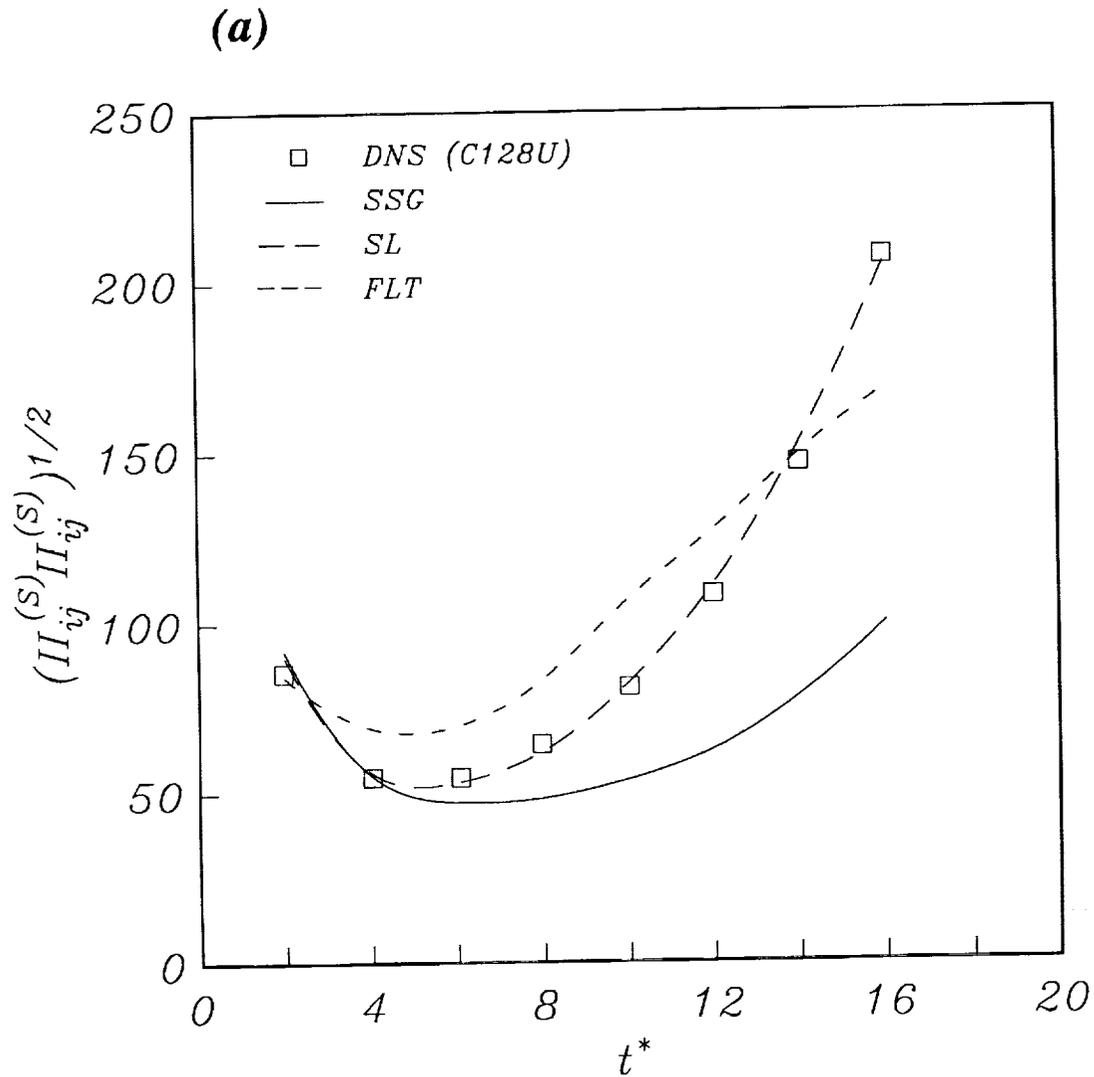
(a)

Figure 1. Comparison of the model predictions for the norm of the pressure-strain correlation with the direct numerical simulation of Rogers *et al.*[8] for homogeneous shear flow (run C128U): (a) slow part, (b) rapid part and (c) total.

(b)

Figure 1. Comparison of the model predictions for the norm of the pressure-strain correlation with the direct numerical simulation of Rogers *et al.*[8] for homogeneous shear flow (run C128U): (a) slow part, (b) rapid part and (c) total.

(c)
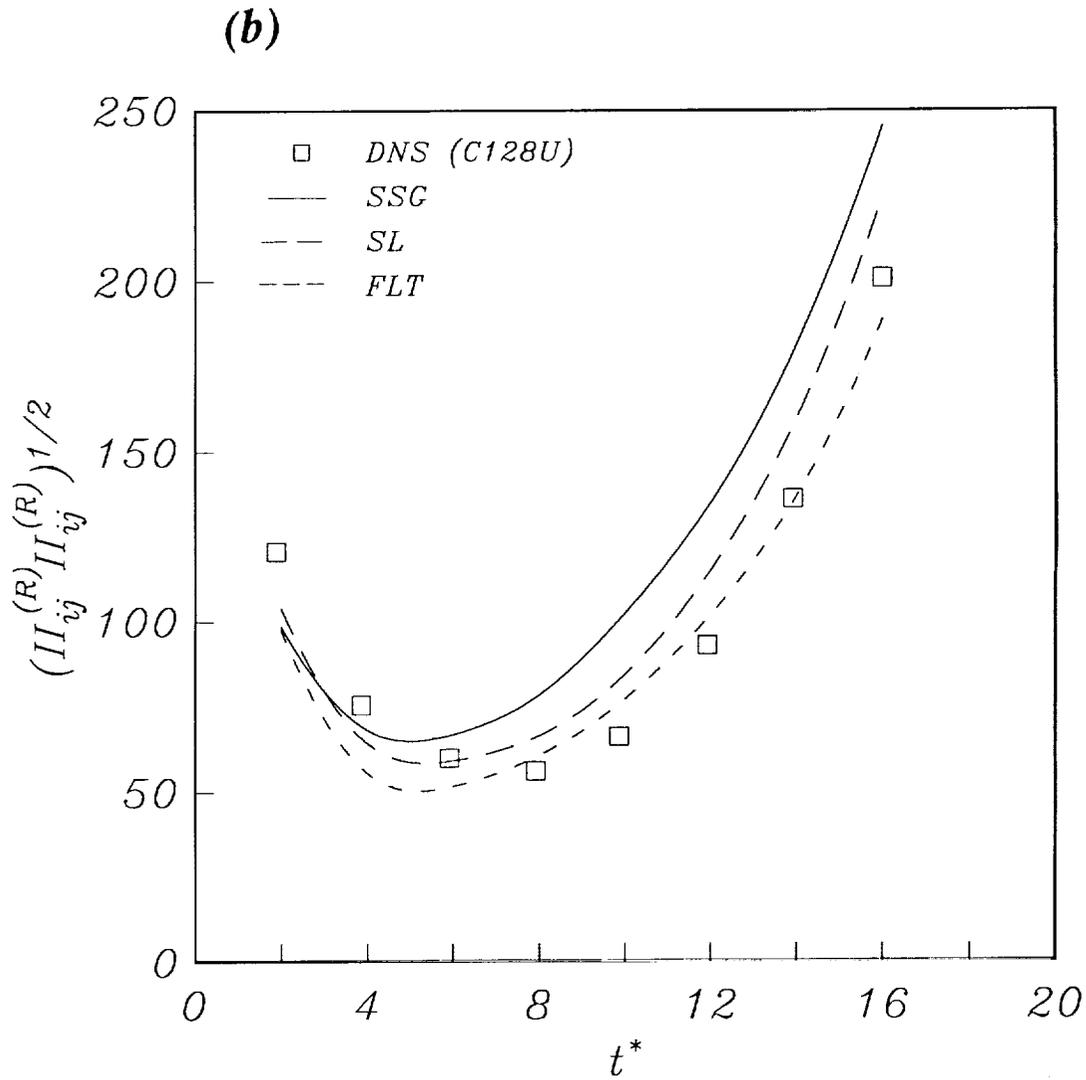
Figure 1. Comparison of the model predictions for the norm of the pressure-strain correlation with the direct numerical simulation of Rogers *et al.*[8] for homogeneous shear flow (run C128U): (a) slow part, (b) rapid part and (c) total.
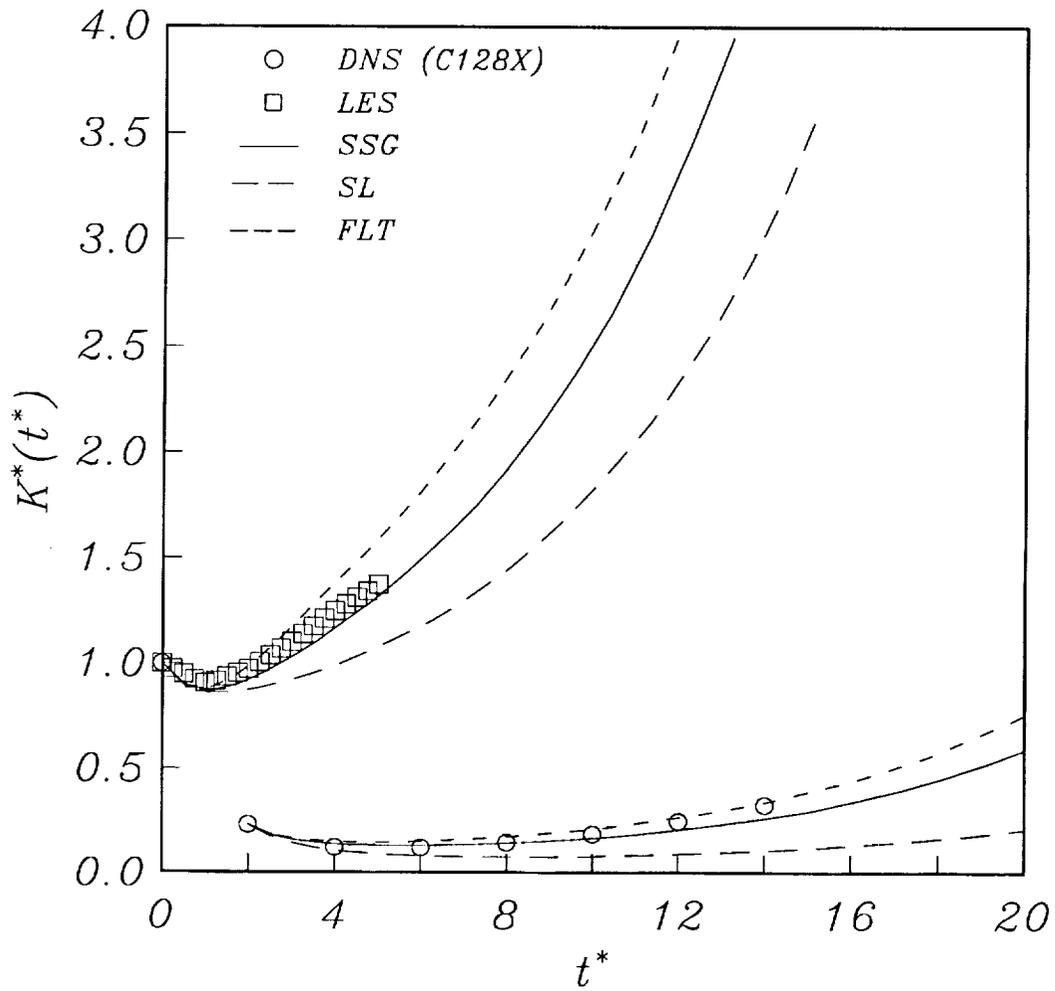
Figure 2. Comparison of the model predictions for the time evolution of the turbulent kinetic energy with the direct numerical simulation of Rogers et al.[8] (run $C128X$) and the large-eddy simulation of Bardina et al.[14] for homogeneous shear flow.
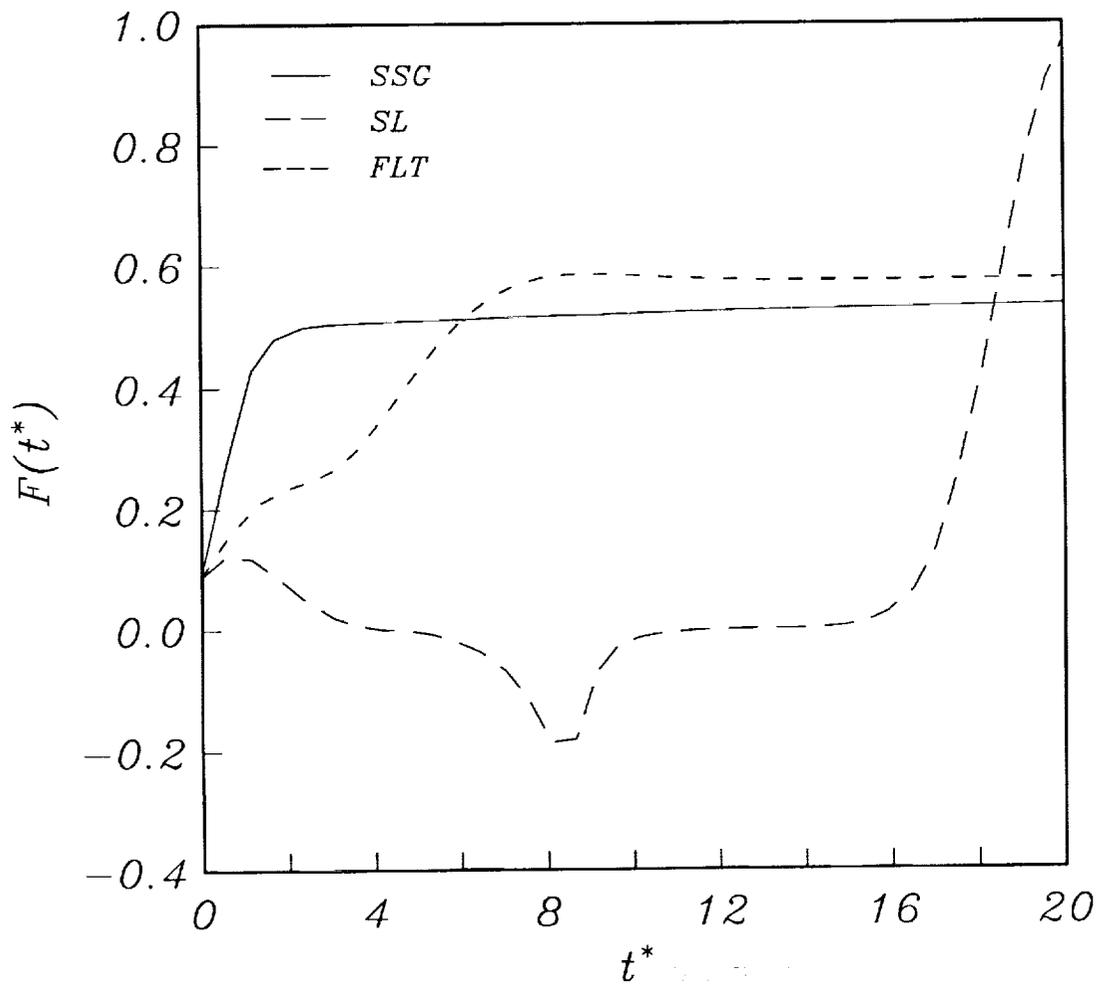
Figure 3. Model predictions for the time evolution of the invariant function $F \equiv 1 + 9II + 27III$ in homogeneous shear flow: $SK_0/\varepsilon_0 = 15$, $(b_{11})_0 = -0.32$ and $(b_{22})_0 = (b_{33})_0 = 0.16$.
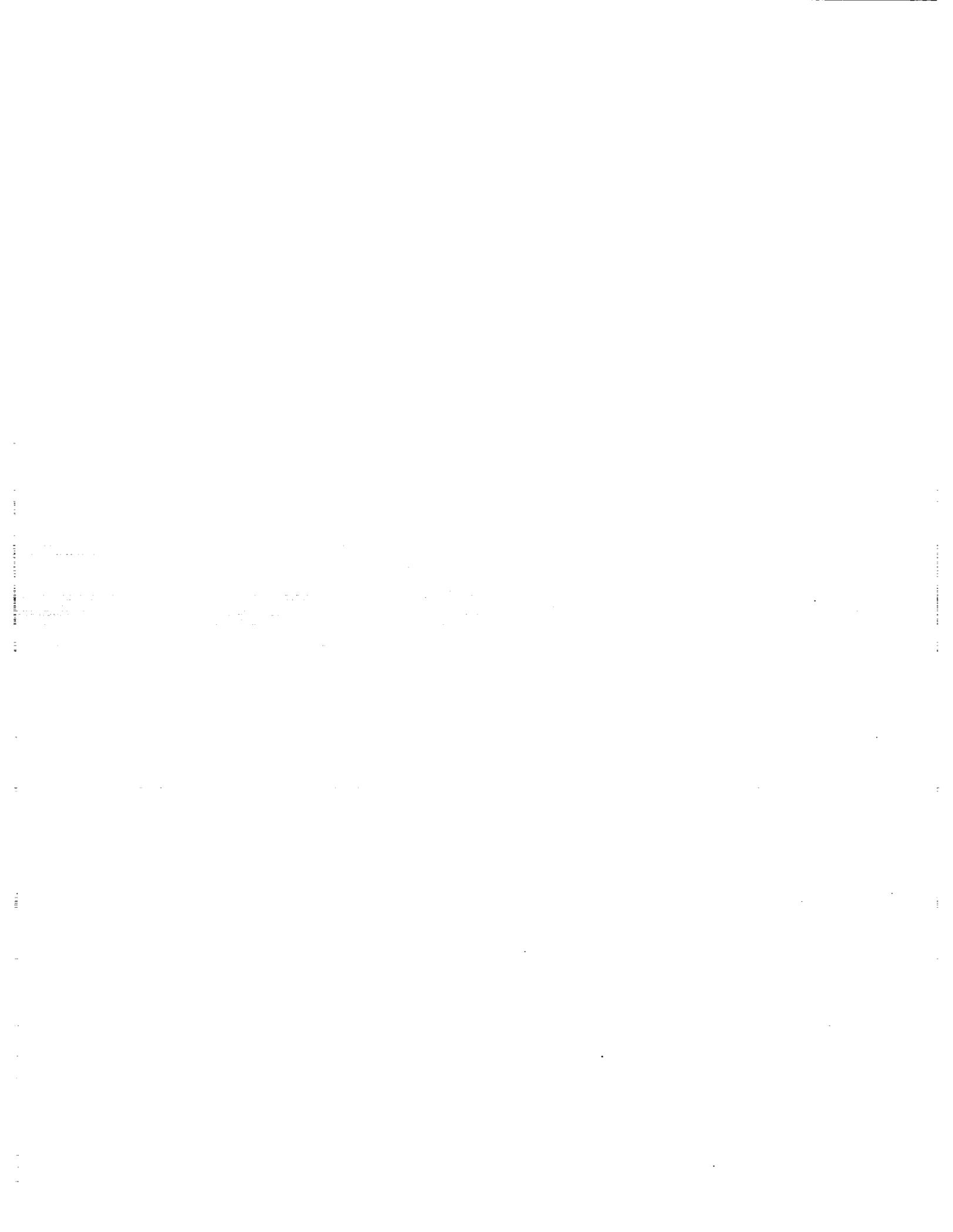
REPORT DOCUMENTATION PAGE

1. AGENCY USE ONLY *(Leave blank)*	2. REPORT DATE March 1994	3. REPORT TYPE AND DATES COVERED Contractor Report

4. TITLE AND SUBTITLE AN ALTERNATIVE ASSESSMENT OF SECOND-ORDER CLOSURE MODELS IN TURBULENT SHEAR FLOWS	5. FUNDING NUMBERS C NAS1-19480 WU 505-90-52-01
6. AUTHOR(S) Charles G. Speziale Thomas B. Gatski	

7. PERFORMING ORGANIZATION NAME(S) AND ADDRESS(ES) Institute for Computer Applications in Science and Engineering Mail Stop 132C, NASA Langley Research Center Hampton, VA 23681-0001	8. PERFORMING ORGANIZATION REPORT NUMBER ICASE Report No. 94-10

9. SPONSORING/MONITORING AGENCY NAME(S) AND ADDRESS(ES) National Aeronautics and Space Administration Langley Research Center Hampton, VA 23681-0001	10. SPONSORING/MONITORING AGENCY REPORT NUMBER NASA CR-194881 ICASE Report No. 94-10

11. SUPPLEMENTARY NOTES

Langley Technical Monitor: Michael F. Card
Final Report
Submitted to AIAA Journal

12a. DISTRIBUTION/AVAILABILITY STATEMENT Unclassified -Unlimited Subject Category 34	12b. DISTRIBUTION CODE

13. ABSTRACT *(Maximum 200 words)*

The performance of three recently proposed second-order closure models is tested in benchmark turbulent shear flows. Both homogeneous shear flow and the log-layer of an equilibrium turbulent boundary layer are considered for this purpose. An objective analysis of the results leads to an assessment of these models that stands in contrast to that recently published by other authors. A variety of pitfalls in the formulation and testing of second-order closure models are uncovered by this analysis.

14. SUBJECT TERMS second-order closure models; homogeneous shear flow; equilibrium turbulent boundary layers	15. NUMBER OF PAGES 20
	16. PRICE CODE A03

17. SECURITY CLASSIFICATION OF REPORT Unclassified	18. SECURITY CLASSIFICATION OF THIS PAGE Unclassified	19. SECURITY CLASSIFICATION OF ABSTRACT	20. LIMITATION OF ABSTRACT